Available online at www.sciencedirect.com
ScienceDirect
Comput. Methods Appl. Mech. Engrg. 383 (2021) 113885
Computer methods in applied mechanics and engineering
www.elsevier.com/locate/cma

A phase field and deep-learning based approach for accurate prediction of structural residual useful life

S.Z. Feng[a,c], Y. Xu[b], X. Han[a,c,*], Z.X. Li[b,d,*], Atilla Incecik[e]

[a] State Key Laboratory of Reliability and Intelligence of Electrical Equipment, Hebei University of Technology, Tianjin, 300130, PR China
[b] School of Engineering, Ocean University of China, Tsingtao, 266100, PR China
[c] School of Mechanical Engineering, Hebei University of Technology, Tianjin, 300130, PR China
[d] Yonsei Frontier Lab, Yonsei University, 50 Yonsei-ro, Seodaemun-gu, Seoul 03722, Republic of Korea
[e] Department of Naval Architecture, Ocean and Marine Engineering, University of Strathclyde, Glasgow, UK

Received 6 February 2021; received in revised form 7 April 2021; accepted 18 April 2021
Available online 15 May 2021

Abstract

In this work, we proposed a novel approach for the prediction of residual useful life (RUL) of structures through appropriately combining the phase field method and deep-learning. In this new approach, the phase field method is firstly utilized to obtain the structural responses of crack growth, which are further preserved as images. Then, the convolutional neural network (CNN) is constructed to establish a predictive model. The proposed approach is a hybrid model of both physical and data-driven techniques, which can build a bridge between traditional computational fracture mechanics and deep learning algorithms. Several numerical cases are studied to evaluate the prediction performance of the proposed approach. The analysis results demonstrate that the present approach is able to predict the RUL of the structures with high level of accuracy.

Keywords: Deep learning; Phase field method; CNN; Residual useful life

1. Introduction

It is nearly impossible to manufacture engineered materials without any initial defects, although the related processing technologies have been greatly developed in the past several years. Material defects, such as voids or cracks, are the main reasons which will greatly reduce the useful life of structures. Therefore, it is of great importance to identify the defect growth mechanisms and perform structural RUL prediction of structures [1,2], which can help to make critical maintenance decision and prevent unprecedented accidents.

Up to today a lot of researches have been done to address the RUL prediction and most of them mainly focused on data-driven approaches [3,4]. For these approaches, a large amount of different kinds of data are collected through sensors and then, machine learning methods are employed to construct the predictive model, which can find the internal connection between the datasets and structural RUL. However, it is difficult to generate sufficient data to feed these data-driven approaches because the cost is too much to carry out physical experiments; and more

* Corresponding authors at: State Key Laboratory of Reliability and Intelligence of Electrical Equipment, Hebei University of Technology, Tianjin, 300130, PR China & School of Engineering, Ocean University of China, Tsingtao 266100, PR China
E-mail addresses: hanxu@hnu.edu.cn (X. Han), zhixiong.li@yonsei.ac.kr (Z.X. Li).

https://doi.org/10.1016/j.cma.2021.113885
0045-7825/

importantly, the data-driven approaches only predict the RUL based on the "black-box" models, which cannot reveal the structural failure mechanisms.

In the past decades, with the rapid development of computer science, numerical methods based on computational mechanics have been successfully applied to crack analysis, such as the boundary element method (BEM) [5–8], meshless method [9–13], finite element method (FEM) [14,15], extended finite element method (XFEM) [16–26], and extended iso-geometric analysis (XIGA) [27–32], which can simulate the crack propagation process in structures during the service life. Among these existing popular numerical methods, the XFEM has become a dominate tool for crack growth analysis, because it can eliminate the remeshing requirement existing in FEM through describing the interior cracks based on enrichment functions. However, it would be very difficult for XFEM to deal with complex crack growth problems, where a crack propagation criterion is always necessary for the analysis. Therefore, in order to deal with crack propagation analysis more flexibly and effectively, Bourdin et al. proposed the variational formulation based on Griffith's theory for brittle fracture analysis, which was the pioneering research of fracture modeling using phase field method [33]. Then, Miehe et al. developed a phase field model with local irreversible constraints for brittle fracture analysis [34–36], which contributed greatly to the study of phase field fracture modeling. Up to now, the phase field method has been successfully extended to many complex crack problems, which can offer great flexibility and convenience for crack modeling [37–45].

Recently, owing to the advancement of machine learning methods [46,47], Rabczuk et al. successfully introduced the Deep Neural Networks (DNNs) into traditional phase field fracture analysis, in which the energy of mechanical systems are utilized as the natural loss function and the final responses of structures can be obtained through training the DNNs [48]. Goswami et al. solved the brittle fracture problems based on phased field method and physics informed neural network (PINN), in which a different path is proposed to minimize the variational energy [49]. In the above mentioned works, the machine learning methods are mainly utilized to directly solve the structural response for fracture analysis. There is another possible way to integrate the phase field method with machine learning methods. Based on phased field fracture analysis, the information of crack and structural responses can be obtained and further preserved as images. By doing so, there are some possibilities to extract intrinsic information from these images to accurately predict the structural RUL.

The artificial neural networks (ANN) have been successfully applied to deal with the image recognition analysis, such as radial basis functions neural networks (RBFNN) [50], convolutional neural networks (CNN) [51], back propagation neural networks (BPNN) [52], etc. Among these methods, the (CNN) has been proved to be a strong tool for image recognition, which is a specific structure of artificial neural network (ANN) and it possesses some unique features to specialize in image recognition applications. In a CNN model, each neuron of the feature map is only sparsely connected to a small portion of neurons in previous layer and this is quite different from traditional neural network structure. This idea is inspired by the concept of simple and complex cells in visual cortex of brain, which contains some cells that are only sensitive to local receptive field [53,54]. Based on this special aforementioned network structure, CNN can effectively accomplish different kinds of image recognition tasks in many fields [55,56]. However, to our best knowledge, CNN has not been used to process phase field images yet. Because the phase field method characterizes the physical process of the structural dynamics, sufficient images can be produced to supply hidden physical patterns of the crack propagation for CNN learning. Thus, CNN is capable to establish a precise predictive model, which is crucial to investigate the hybrid model of phase field and CNN for structural RUL prediction.

This work attempts to build a bridge between two distinct fields (i.e., computational mechanics and machine learning fields) by presenting a novel approach that appropriately combines the phase field method and CNN. The phase field method is employed to generate sufficient images associated with the structural responses and RUL. Then, a CNN prediction model is constructed through learning these images. Lastly, the well-trained CNN model is utilized to predict RUL from new testing images and the obtained results demonstrate that the proposed approach is able to achieve high level of predication accuracy.

This paper is organized as follows. In Section 2, the crack propagation analysis based on phase field method is briefly introduced. In Section 3, the construction of CNN prediction model is described. In Section 4, several numerical cases are studied to fully evaluate the performance of the proposed approach. Some concluding remarks are presented in Section 5.

2. Phase field method for crack growth analysis

A brief discussion of the phase field formulation will be present in this section. According to the variational theory of fracture, the cracks always grow in the way that the total system energy is minimized and the total energy of a system containing cracks is expressed as

$$\Pi = \Psi_e(\boldsymbol{\varepsilon}) + \Psi_f - \Psi_{ext}(\mathbf{u}) \tag{1}$$

Where, $\Psi_e(\boldsymbol{\varepsilon})$ represents the elastic strain energy, Ψ_f denotes the fracture surface energy caused by cracks and $\Psi_{ext}(\mathbf{u})$ represents the external potential energy, which is defined as

$$\Psi_f = g_c \int_\Omega \gamma(c) d\Omega \tag{2}$$

where g_c is the critical energy release rate, c denotes the phase field parameter and $\gamma(c)$ represents the density function, which is calculated by

$$\gamma(c) = \frac{1}{2}\left[\frac{1}{l_c}c^2 + \frac{l_c}{2}|\nabla c|^2\right] \tag{3}$$

where l_c denotes the length scale parameter.

For a system with cracks, the total internal potential energy is consisted of the bulk energy and the energy required for the formation of cracks, which is expressed as

$$\Psi(u,c) = \int_\Omega [(1-c)^2 + d]\Psi_e(\boldsymbol{\varepsilon}) d\Omega + \int_\Omega \frac{g_c}{2}[l_c \nabla c \cdot \nabla c + \frac{1}{l_c}c^2] d\Omega \tag{4}$$

where the parameter d is utilized to ensure the numerical stabilization.

Based on the variation of the energy potentials and employing the principal of virtual displacements, the following governing equations can be obtained

$$\text{displacement field}: \begin{cases} \nabla \cdot \boldsymbol{\sigma} + \overline{\boldsymbol{\gamma}} = 0 & \text{in } \Omega \\ \mathbf{u} = \overline{\mathbf{u}} & \text{on } \Gamma_u \\ \boldsymbol{\sigma} \cdot \mathbf{n} = \bar{\mathbf{t}} & \text{on } \Gamma_t \end{cases} \tag{5}$$

$$\text{phase field}: \begin{cases} g_c\left(\frac{1}{l_c}c - l_c\nabla^2 c\right) = 2(1-c)\,\mathrm{H} & \text{in } \Omega \\ \nabla c \cdot \mathbf{n} = 0 & \text{on } \Gamma_c \end{cases} \tag{6}$$

where $\overline{\boldsymbol{\gamma}}$ and $\bar{\mathbf{t}}$ denote the body and face forces, respectively. $\mathrm{H} = \max\left(\Psi_e(\boldsymbol{\varepsilon})^+\right)$ is the history parameter, more detailed calculation procedures of this parameter can be found in [35].

After the finite element discretization process, the following system equations can be obtained as

$$\int_\Omega [(1-c)^2 + d](\mathbf{B}_u)^T \boldsymbol{\sigma} d\Omega = \int_\Gamma (\mathbf{N}_u)^T \overline{\boldsymbol{\gamma}} d\Gamma + \int_\Gamma (\mathbf{N}_u)^T \bar{\mathbf{t}} d\Gamma \tag{7}$$

$$\int_\Omega [g_c l_c (\mathbf{B}_c)^T \nabla c + (\frac{g_c}{l_c} + 2\mathrm{H})(\mathbf{N}_c)^T c] d\Omega = \int_\Omega 2\mathrm{H}(\mathbf{N}_c)^T d\Omega \tag{8}$$

where $\mathbf{N}$ is the FEM shape function matrix and $\mathbf{B}$ denotes the gradient matrix. For crack growth analysis, the above coupled nonlinear system equation can be solved through Newton–Raphson iteration, which is expressed as

$$\begin{Bmatrix} c \\ \mathbf{u} \end{Bmatrix}_{n+1} = \begin{Bmatrix} c \\ \mathbf{u} \end{Bmatrix}_n - \begin{bmatrix} \mathbf{K}_c & 0 \\ 0 & \mathbf{K}_u \end{bmatrix}_n^{-1} \begin{Bmatrix} \mathbf{R}_c \\ \mathbf{R}_u \end{Bmatrix}_n \tag{9}$$

where,

$$\mathbf{K}_u = \int_\Omega [(1-c)^2 + d](\mathbf{B}_u)^T \mathbf{D}(\mathbf{B}_u) d\Omega \tag{10}$$

$$\mathbf{K}_c = \int_\Omega [g_c l_c (\mathbf{B}_c)^T (\mathbf{B}_c) + (\frac{g_c}{l_c} + 2\mathrm{H})(\mathbf{N}_c)^T (\mathbf{N}_c)] d\Omega \tag{11}$$

$$\mathbf{R}_c = \int_\Omega 2\mathrm{H}(\mathbf{N}_c)^T d\Omega - \int_\Omega [g_c l_c (\mathbf{B}_c)^T \nabla c + (\frac{g_c}{l_c} + 2\mathrm{H})(\mathbf{N}_c)^T c] d\Omega \tag{12}$$

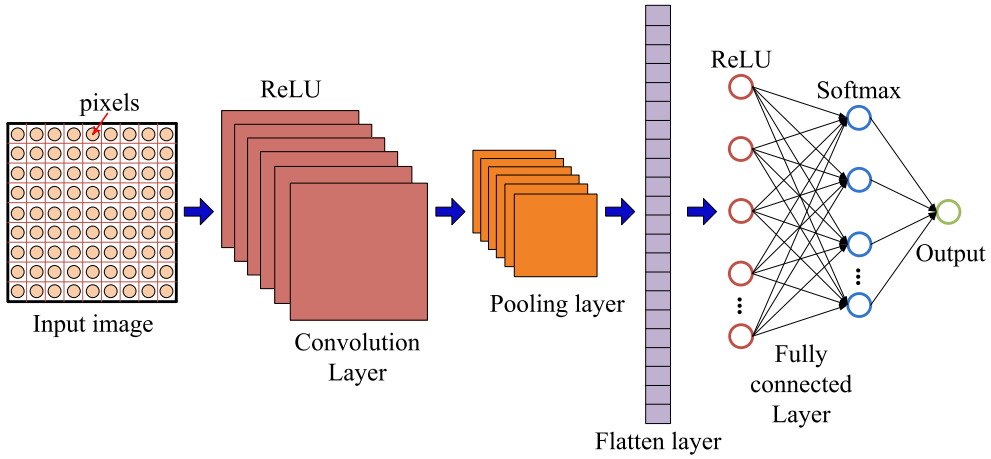

Fig. 1. Description of the topology structure of CNN.

$$\mathbf{R}_u = \int_\Gamma (\mathbf{N}_u)^T \overline{\boldsymbol{\gamma}} d\Gamma + \int_\Gamma (\mathbf{N}_u)^T \bar{\mathbf{t}} d\Gamma - \int_\Omega [(1-c)^2 + d](\mathbf{B}_u)^T \boldsymbol{\sigma} d\Omega \tag{13}$$

The above equations can be solved by making $\mathbf{R}_c = 0$ and $\mathbf{R}_u = 0$ in a staggered system. The Newton–Raphson method is employed in this work to solve the above nonlinear equations. Note that some other methods have also been proposed to solve these equations, such as BFGS [57], which can achieve high level of efficiency. It is very convenient to describe the cracks using the phase field parameter and the crack propagation process can be easily tracked. In each calculation step, the obtained information of displacement field and phase field will be preserved in the form of images. These images are associated with the details of RUL of structures and will be further utilized to construct the CNN predictive model.

3. CNN predictive model

3.1. Brief discussion of CNN

CNN is a popular type of deep neural network, which is utilized to deal with images, which possesses a special way to extract distinct information from the images. A typical five-layered structure of CNN is illustrated in Fig. 1. Each layer of the CNN is briefly discussed as follows.

(a) Convolution Layer. This layer is the core layer of CNN, which is composed of many filters. These filters are of small size and are utilized to perform dot product operation with the image pixels. The convolution operation can be mathematically expressed as

$$z_j^l = f\left(x_i^{l-1} * w_{ij}^{(1)l} + b_j^{(1)l}\right) \tag{14}$$

where, x_i^{l-1} denotes the image pixels, f is the activation function, $b_j^{(1)l}$ represents the bias of lth layer, $w_{ij}^{(1)l}$ is the convolution kernel matrix for lth layer.

(b) Pooling layer. The down-sampling operation is mainly performed in this layer, which usually follows the convolutional layer to further merge the features. This layer has no parameters and utilized one specific value to represent the compositive features. There are mainly two representative pooling operations including the max and average pooling. In this work, the max pooling operation was employed.

(c) Flatten layer. The multi-dimensional data is converted to one-dimensional data in this layer, which is mainly employed between the convolution Layer and the Fully connected Layer.

(d) Fully connected Layer. In this layer, the neurons are connected to every neuron in the subsequent layer, which is very similar to the structure of a traditional neural network. The operation is mathematically described as

$$z_j^l = f\left(z_i^{l-1} * w_{ij}^{(2)l} + b_j^{(2)l}\right) \tag{15}$$

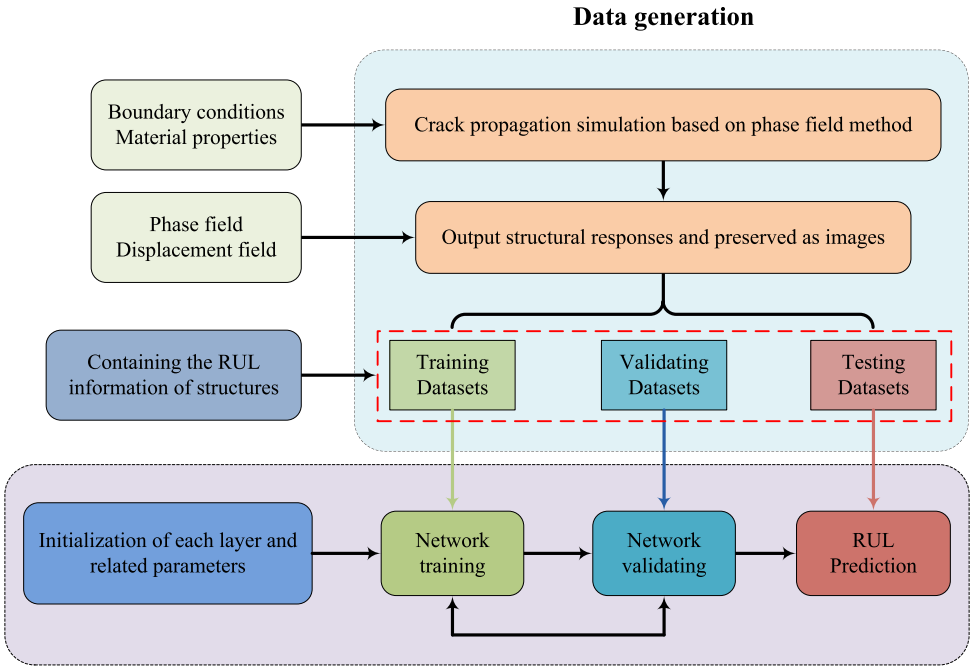

Fig. 2. Brief description of the overall approach.

where, z_i^{l-1} denotes the input from the previous layer, f is also the activation function, $b_j^{(2)l}$ is the bias and $w_{ij}^{(2)l}$ represents the weight coefficient.

(e) Softmax function layer. The probabilities distribution of a target class over all possible classes is calculated in this layer and it is expressed as

$$P\left(y_j^l\right) = \frac{\exp\left(y_j^l\right)}{\sum_{j=1}^{k} \exp\left(y_j^l\right)} \tag{16}$$

3.2. RUL prediction based on CNN

The main idea of this approach is to integrate the phase field method with CNN, which can save huge amount of cost caused by physical experiments. The phase field method is utilized to effectively track the crack propagation process of engineering structures and the information of structural responses associated with the RUL of structures are preserved in the form of images. These images are separated and further put into training, validating and testing datasets, respectively.

Then, we initially construct the CNN with different layer as discussed in Fig. 1. It should be noted that the ReLU activation function is used in the related layers of the CNN. In addition, the training datasets are utilized to optimize the related coefficients of the CNN layers, while the validating datasets are employed to inspect the performance of the CNN. Finally, the testing datasets are used to verify the performance of well-trained CNN model and it is realized that the RUL of the structures can be predicted in a real-time manner based on the proposed approach. An overview of the proposed approach is presented in Fig. 2.

4. Results and discussion

In this section, two case studies are investigated to evaluate the performance of proposed approach. The structure of the CNN model in this work is mainly based on the classical LeNet-5 proposed by LeCun et al. [58]. First,

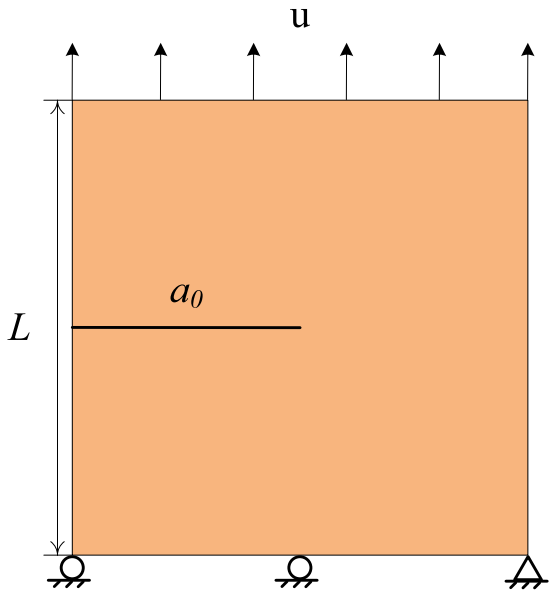

Fig. 3. Schematic of an infinite plate with center crack.

there are two convolution layers and each of them is followed by one max pooling layer. Then, there is a flatten layer and two fully connected layers with the ReLU and Softmax functions, respectively. The structure of classical LeNet-5 is not complex and it can solve many problems through the optimization of network parameters. The Batch Normalization, Data Augmentation and Dropout technique are also employed, which can successfully settle the over-fitting problems and improve the performance on the testing datasets, not only on the training datasets. In addition, the displacement of structures is very easy to measure by using commercial sensors, and hence, we mainly use the distributions of structural displacements obtained by the phase field method to train the CNN model. In order to update the large amount of parameters of CNN, the cross-entropy function is employed as the loss function [59], which is expressed as

$$loss = -\sum_{j=1}^{m}(y_j^T)\ln(y_j^p) \tag{17}$$

where y^P is the prediction value of CNN, y^T represents the target value.

4.1. Case 1

A square plate with a horizontal crack is first studied to investigate the performance of present approach in this section, as shown in Fig. 3. The related parameters in the computation are given as: $L = 1.0$ mm, initial crack $a_0 = 0.5$ mm, $E = 210$ kN/mm ^{2}, $\nu = 0.3$, $g_c = 2.7\times10^{-3}$ kN/mm, $l_c = 0.0075$ mm. A displacement increment of du=1×10^{-5} mm is applied on the top edge. In each crack propagation step, the corresponding structural responses are all preserved as images, which are associated with the RUL of structures. In this case, there are 1000 calculation steps in total and they are further divided into 20 intervals, which refer to different RUL of structure. It should be noted that there is no particular reason to divide the datasets into 20 intervals and it just represents the number of labels for these datasets. The information of 600 steps is used to generated training datasets, 160 steps are used for validation purpose and the other 240 steps are employed to create the testing datasets.

At first, the computational mesh and evolution of crack are described in Fig. 4. The load–displacement curve is compared with previous work [60], as shown in Fig. 5, based on which the effectiveness of our computed results can be well ensured. Then, we begin to train the CNN model based on images of displacement field. In order to implement the image recognition process, the values of the displacement field are mapped through logarithm function. During the training process, the variations of predictive accuracy and loss function for training

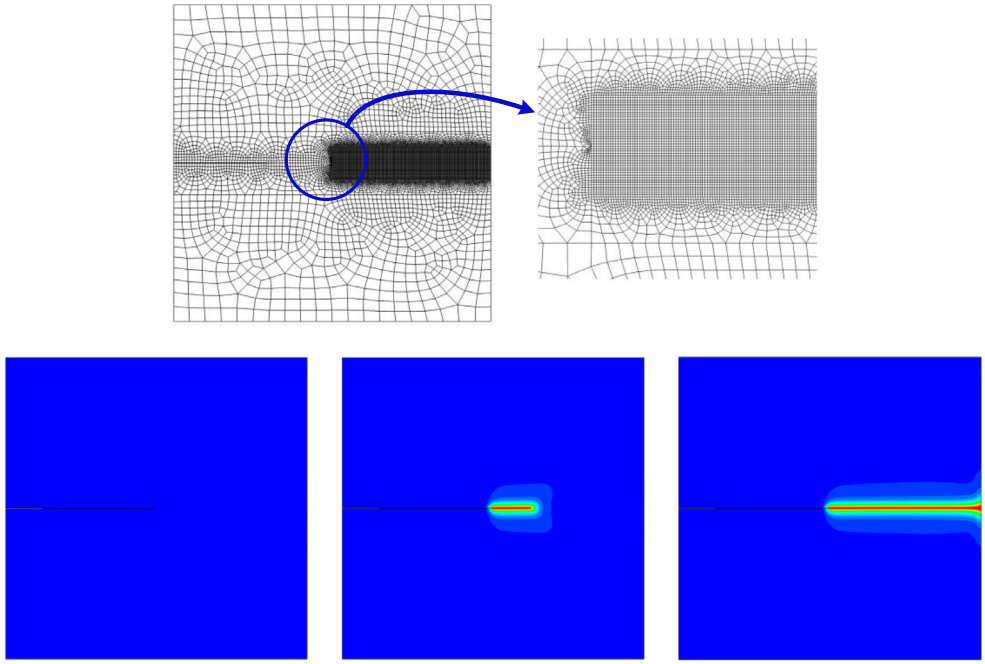

Fig. 4. Description of the computational mesh and crack propagation process.

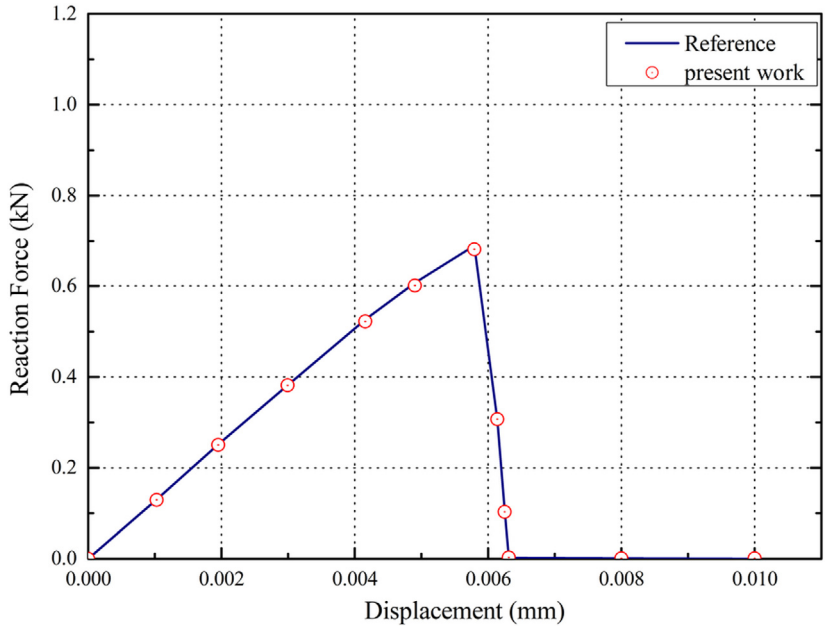

Fig. 5. Comparison of load–displacement curve.

datasets and validating datasets are given in Figs. 6 and 7, respectively. After 200 iterations, it is observed that the accuracy of training datasets is about 94.2% and the accuracy of validating datasets is about 98.8%. The values of loss function for training datasets and validating datasets all become very small. Therefore, the CNN model has been well trained and no obvious over-fitting phenomenon is observed. The trained CNN model can be further utilized to make predictions for testing datasets.

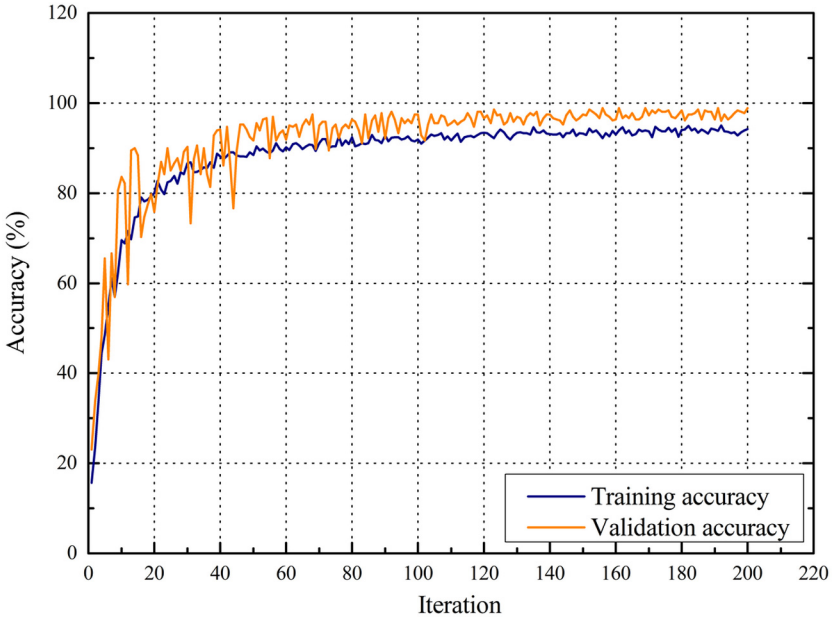

Fig. 6. The variation of training and validation accuracy.

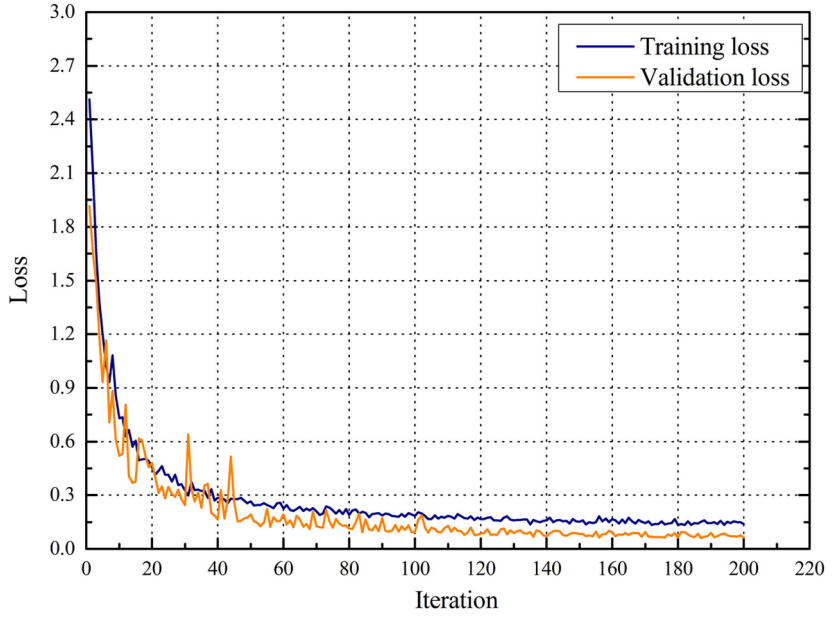

Fig. 7. The variation of training and validation loss.

We train the CNN model for 10 times and the accuracy for each trial is listed in Table 1. It is found that the mean accuracy of the CNN model is 98.45% and it may reach above 99% in some trials. These results demonstrate that almost all the images associated RUL of structure can be accurately classified and the related RUL of structures can be effectively predicted. The best performance is achieved in No. 6 trial and the confusion matrix for this trial is presented in Fig. 8, in which the columns stand for the true label and the rows stand for the predicted label. As can be seen, most of the diagonal element is equal to 1, which means the trained CNN model can achieve 100% prediction accuracy.

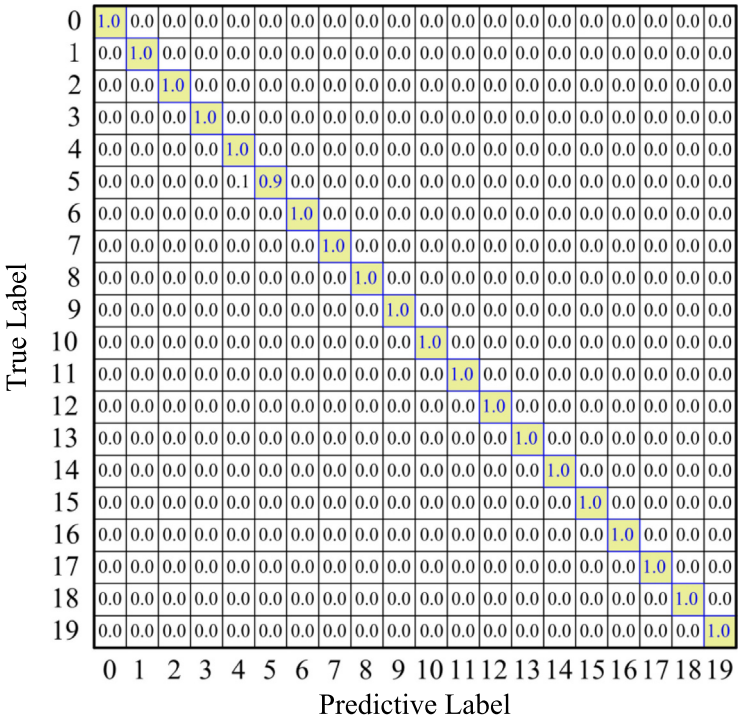

Fig. 8. The obtained confusion matrix for trial No. 3.

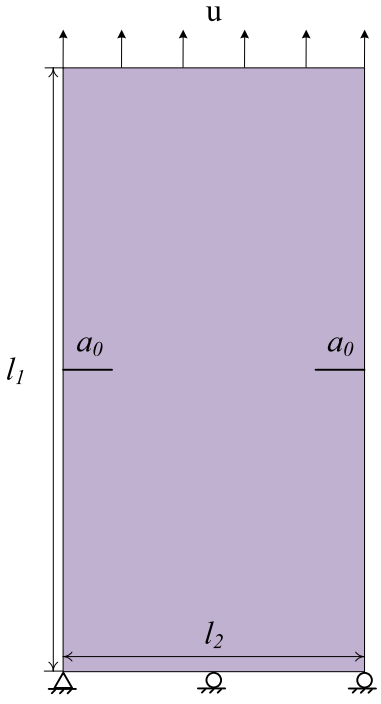

Fig. 9. Illustration of a plate containing double edge crack.

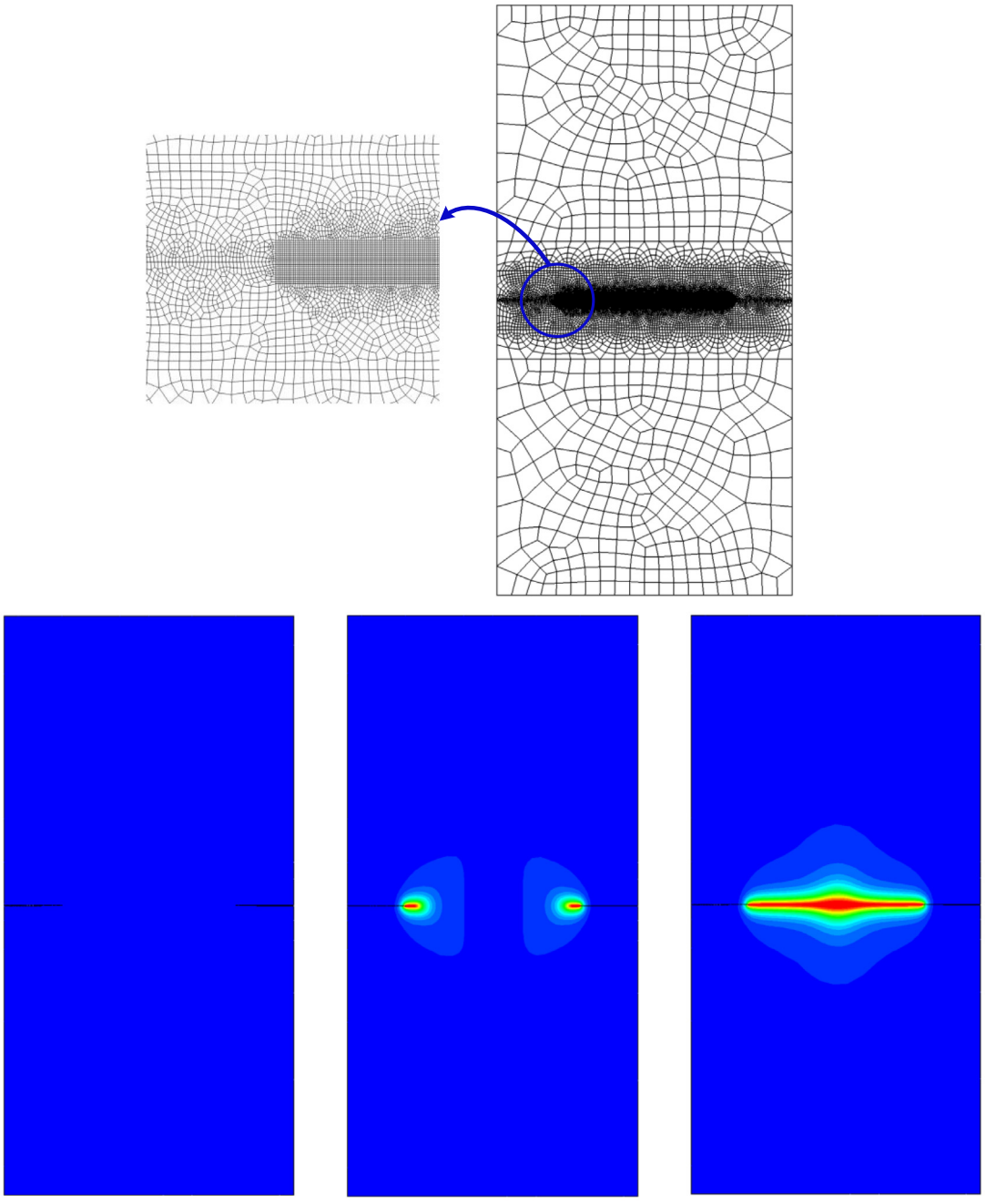

Fig. 10. Description of the computational mesh and crack propagation process.

Table 1
The predictive accuracy of CNN model for different trials.

No.	1	2	3	4	5	6	7	8	9	10
CNN accuracy	98.0%	98.5%	98.0%	98.5%	99.0%	99.5%	98.5%	97.5%	98.5%	98.5%

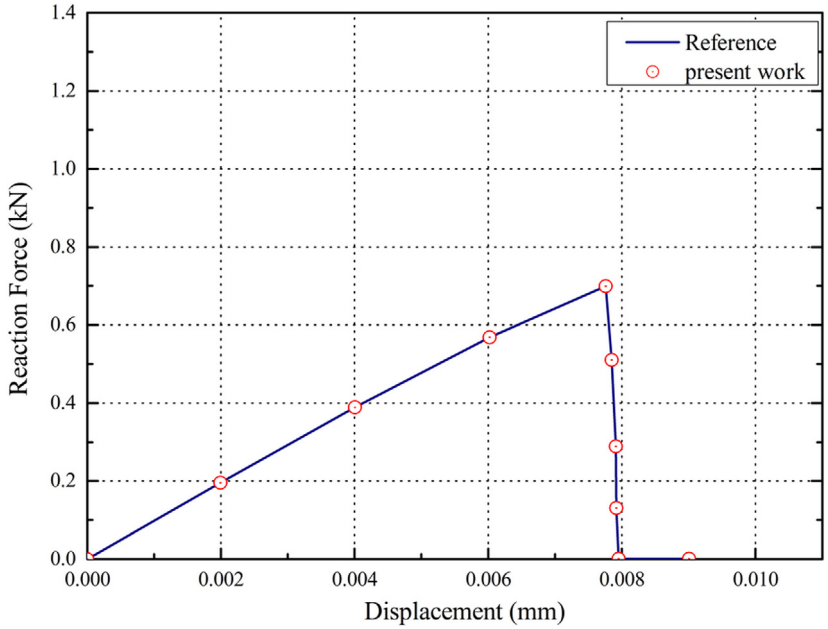

Fig. 11. Comparison of load–displacement curve.

Table 2
The predictive accuracy of CNN model for different trials.

No.	1	2	3	4	5	6	7	8	9	10
CNN accuracy	98.90%	99.30%	99.00%	99.15%	99.20%	99.15%	99.00%	99.30%	99.55%	98.95%

4.2. Case 2

A double notched plate with edge cracks is examined in this section, as illustrated in Fig. 9. The geometric parameters of the plate are given as: $l_1 = 1$ mm, $l_2 = 0.5$ mm, initial crack length $a_0 = 0.1$ mm. The other parameters involved in the computation are listed as: $E = 210$ kN/mm^2, $\nu = 0.3$, $g_c = 2.7\times10^{-3}$ kN/mm, $l_c = 0.0075$ mm. A displacement increment of du=1×10^{-6} mm is applied on the top edge. In this case, there are 10000 crack propagation steps in total, which are also divided into 20 RUL intervals. The images of 6000 steps are utilized to generate the training datasets, 1600 steps are employed for the validation analysis and the other 2400 steps are used for the final testing purpose.

Firstly, the computational mesh and crack growth process are given in Fig. 10. The load–displacement curve of present work is also compared with the published work [60], as depicted in Fig. 11, which can ensure the effectiveness of our computed results. Then, we start to construct the CNN predictive model based on the obtained images of displacement field. For the training process of CNN, the variations of predictive accuracy and loss function for training and validating datasets are respectively plotted in Figs. 12 and 13. It can be seen that the accuracy of training and validating datasets are about 96.16% and 99.00%, respectively. The values of loss function for training and validating datasets also achieve a very low level. No obvious over-fitting phenomenon is observed and hence the trained CNN model can be further employed for the predictions of testing datasets.

The CNN model is trained and validated for 10 times in this case and the predictive accuracy for these trials are given in Table 2. It is observed that the mean accuracy of CNN model can achieve 99.15% and the best performance is 99.55% in No. 9. For this trial, the confusion matrix is given in Fig. 14, from which it can be seen that only a few portions of these images associated with the RUL of structures in testing datasets are misclassified, which again verify that the proposed approach can provide good performance and has the ability to intelligently predict the RUL of structures with high accuracy.

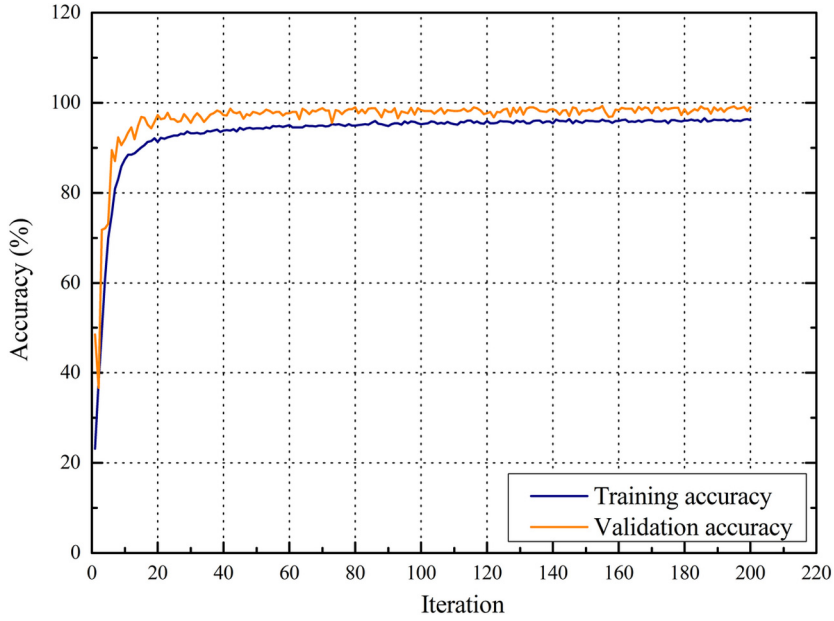

Fig. 12. The variation of training and validation accuracy.

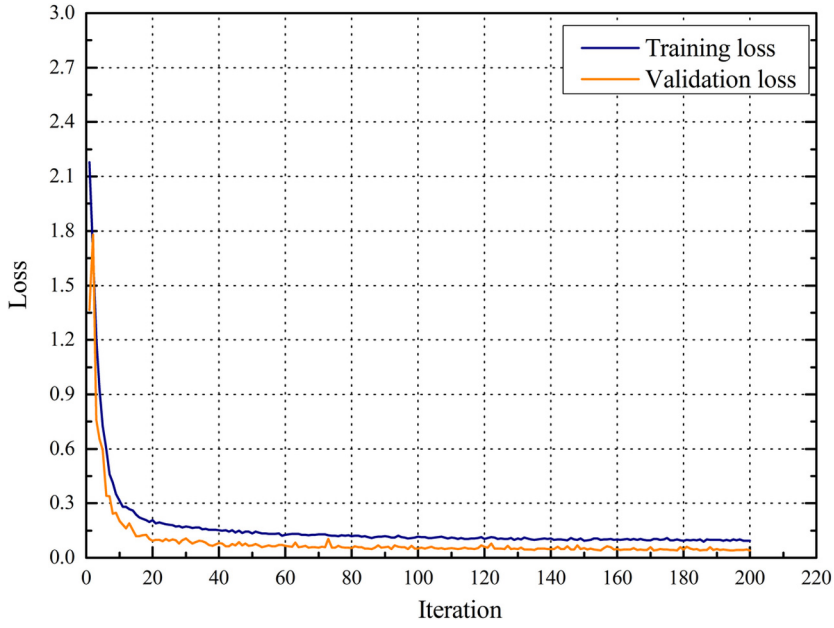

Fig. 13. The variation of training and validation accuracy.

5. Conclusion

In this study, a feasible approach for the RUL prediction of structures is proposed through combining the phase field method and CNN, which shows good performance during the test. This new approach can build a new bridge between traditional computational fracture mechanics and Artificial intelligence method. It can not only take the advantage of phase field method when deal with crack analysis, but also can realize the intelligent RUL prediction

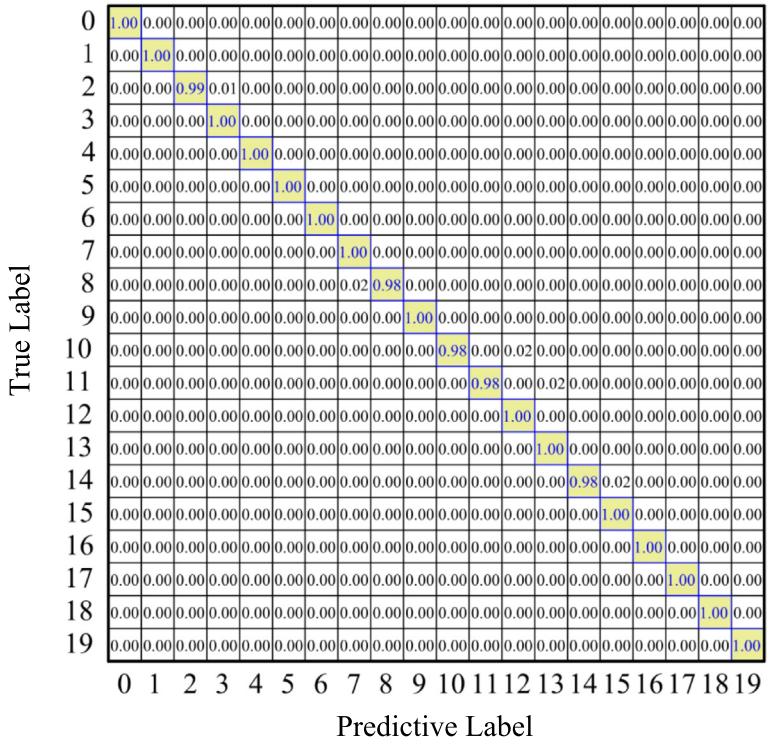

Fig. 14. The obtained confusion matrix for trial No. 6.

of structures based on CNN model. Two case studies are investigated to fully evaluate the performance of proposed approach. Based on these studies, main conclusions can be drawn as:

1. The proposed approach can effectively track the evolution of cracks and obtain images associated with the RUL information of structures, which can save huge amount of experimental cost.
2. The constructed CNN predictive model can make accurate predictions after proper training and validation process.
3. The performance can be further improved through adjusting the framework of CNN networks, which will be done in future study.

In addition, our future work will focus on extending this approach to the RUL prediction of three-dimensional structures and the related technique of measurement will also be studied.

Declaration of competing interest

The authors declare that they have no known competing financial interests or personal relationships that could have appeared to influence the work reported in this paper.

Acknowledgments

This work is supported by the Natural Science Foundation of Hebei Province of China (A2020202017), Youth Foundation of Hebei Education Department, China (QN2020211), Major Scientific and Technological Innovation Project of Shandong Province of China (No. 2019JZZY010820) and foundation strengthening program, China (No: 2019-JCJQ-00).

References

[1] J.V. Sahadi, D. Nowell, R.J.H. Paynter, Fatigue life prediction for waspaloy under biaxial loading, Theor. Appl. Fract. Mech. 97 (2018) 1–14.

[2] P. Ding, H. Wang, W.G. Bao, R.J. Hong, HYGP-MSAM based model for slewing bearing residual useful life prediction, Measurement 141 (2019) 162–175.

[3] Z.Z. Pan, Z. Meng, Z.J. Chen, W.Q. Gao, Y. Shi, A two-stage method based on extreme learning machine for predicting the remaining useful life of rolling-element bearings, Mech. Syst. Signal Process. 144 (2020) 106899.

[4] D.M. Francesco, L.T. Kwok, Z. Enrico, Combining relevance vector machines and exponential regression for bearing residual life estimation, Mech. Syst. Signal Process. 31 (2012) 405–427.

[5] X. Peng, E. Atroshchenko, E. Atroshchenko, P. Kerfriden, S.P.A. Bordas, Isogeometric boundary element methods for three dimensional static fracture and fatigue crack growth, Comput. Methods Appl. Mech. Engrg. 316 (2017) 151–185.

[6] B.H. Nguyen, H.D. Tran, C. Anitescu, X. Zhuang, T. Rabczuk, An isogeometric symmetric Galerkin boundary element method for two-dimensional crack problems, Comput. Methods Appl. Mech. Engrg. 306 (2016) 252–275.

[7] W. Zhou, B. Liu, Q. Wang, X.L. Chang, X.D. Chen, Formulations of displacement discontinuity method for crack problems based on boundary element method, Eng. Anal. Bound. Elem. 155 (2020) 86–95.

[8] G.Z. Xie, F.L. Zhou, D.H. Zhang, X.Y. Wen, H. Li, A novel triangular boundary crack front element for 3D crack problems based on 8-node serendipity element, Eng. Anal. Bound. Elem. 105 (2019) 296–302.

[9] Y.C. Cai, P. Sun, H.H. Zhu, T. Rabczuk, A mixed cover meshless method for elasticity and fracture problems, Theor. Appl. Fract. Mech. 95 (2018) 73–103.

[10] T. Rabczuk, T. Belytschko, Cracking particles: A simplified meshfree method for arbitrary evolving cracks, Internat. J. Numer. Methods Engrg. 13 (2004) 2316–2343.

[11] T. Rabczuk, T. Belytschko, Three-dimensional large deformation meshfree method for arbitrary evolving cracks, Comput. Methods Appl. Mech. Engrg. 29–30 (2007) 2777–2799.

[12] T.Q. Bui, N.T. Nguyen, L.V. Lich, M.N. Nguyen, T.T. Truong, Analysis of transient dynamic fracture parameters of cracked functionally graded composites by improved meshfree methods, Theor. Appl. Fract. Mech. 96 (2018) 642–657.

[13] N.T. Nguyen, T.Q. Bui, C.Z. Zhang, T.T. Truong, Crack growth modeling in elastic solids by the extended meshfree Galerkin radial point interpolation method, Eng. Anal. Bound. Elem. 44 (2014) 87–97.

[14] L. Chen, G.R. Liu, N.N. Nourbakhsh, K. Zeng, A singular edge-based smoothed finite element method (ES-FEM) for bimaterial interface cracks, Comput. Mech. 45 (2010) 109–125.

[15] H. Nguyen-Xuan, G.R. Liu, S. Bordas, S. Natarajan, T. Rabczuk, An adaptive singular ES-FEM for mechanics problems with singular field of arbitrary order, Comput. Methods Appl. Mech. Engrg. 253 (2013) 252–273.

[16] S.Z. Feng, X. Han, A novel multi-grid based reanalysis approach for efficient prediction of fatigue crack propagation, Comput. Methods Appl. Mech. Engrg. 353 (2019) 107–122.

[17] T. Belytschko, T. Black, Elastic crack growth in finite elements with minimal remeshing, Internat. J. Numer. Methods Engrg. 45 (5) (1999) 601–620.

[18] N. Sukumar, N. Moes, B. Moran, T. Belytschko, Extended finite element method for three-dimensional crack modelling, Internat. J. Numer. Methods Engrg. 48 (11) (2000) 1549–1570.

[19] I.V. Singh, B.K. Mishra, S. Bhattacharya, R.U. Patil, The numerical simulation of fatigue crack growth using extended finite element method, Int. J. Fatigue 36 (2012) 109–119.

[20] S.Z. Feng, S.P.A. Bordas, X. Han, G. Wang, Z.X. Li, A gradient weighted extended finite element method (GW-XFEM) for fracture mechanics, Acta Mech. 230 (2019) 2385–2398.

[21] L. Chen, T. Rabczuk, S. Bordas, G.R. Liu, K.Y. Zeng, P. Kerfriden, Extended finite element method with edge-based strain smoothing (ESm-XFEM) for linear elastic crack growth, Comput. Methods Appl. Mech. Engrg. 209 (2012) 250–265.

[22] Sachin Kumar, I.V. Singh, B.K. Mishra, T. Rabczuk, Modeling and simulation of kinked cracks by virtual node XFEM, Comput. Methods Appl. Eng. 283 (2015) 1425–1466.

[23] R.U. Patil, B.K. Mishra, I.V. Singh, A new multiscale XFEM for the elastic properties evaluation of heterogeneous materials, Int. J. Mech. Sci. 122 (2017) 277–287.

[24] S.Z. Feng, W. Li, An accurate and efficient algorithm for the simulation of fatigue crack growth based on XFEM and combined approximations, Appl. Math. Model. 55 (2018) 600–615.

[25] T.T. Yu, T.Q. Bui, Numerical simulation of 2-D weak and strong discontinuities by a novel approach based on XFEM with local mesh refinement, Comput. Struct. 196 (2018) 112–133.

[26] T.Q. Bui, M.N. Nguyen, N.T. Nguyen, T.T. Truong, L.V. Lich, Simulation of dynamic and static thermoelastic fracture problems by extended nodal gradient finite elements, Int. J. Mech. Sci. 134 (2017) 370–386.

[27] S.S. Ghorashi, N. Valizadeh, S. Mohammadi, Extended isogeometric analysis for simulation of stationary and propagating cracks, Internat. J. Numer. Methods Engrg. 89 (9) (2011) 1069–1101.

[28] S. Ghorashi, N. Valizadeh, S. Mohammadi, T. Rabczuk, T-spline based XIGA for fracture analysis of orthotropic media, Comput. Struct. 147 (2015) 138–146.

[29] T.Q. Bui, Extended isogeometric dynamic and static fracture analysis for cracks in piezoelectric materials using NURBS, Comput. Methods Appl. Mech. Engrg. 295 (2015) 470–509.

[30] T. Yu, T.Q. Bui, S. Yin, D.H. Doan, C. Wu, T.V. Do, S. Tanaka, On the thermal buckling analysis of functionally graded plates with internal defects using extended isogeometric analysis, Compos. Struct. 136 (2016) 684–695.

[31] G. Bhardwaj, I. Singh, B. Mishra, T. Bui, Numerical simulation of functionally graded cracked plates using NURBS based XIGA under different loads and boundary conditions, Compos. Struct. 126 (2015) 347–359.
[32] G. Bhardwaj, I. Singh, B. Mishra, Stochastic fatigue crack growth simulation of interfacial crack in bi-layered FGMs using XIGA, Comput. Methods Appl. Mech. Engrg. 284 (2015) 186–229.
[33] B. Bourdin, G.A. Francfort, J.J. Marigo, Numerical experiments in revisited brittle fracture, J. Mech. Phys. Solids 48 (2000) 797–826.
[34] C. Miehe, F. Welschinger, M. Hofacker, Thermodynamically consistent phase-field models of fracture: Variational principles and multi-field fe implementations, Internat. J. Numer. Methods Engrg. 83 (10) (2010) 1273–1311.
[35] C. Miehe, M. Hofacker, F. Welschinger, A phase field model for rate-independent crack propagation: Robust algorithmic implementation based on operator splits, Comput. Methods Appl. Mech. Engrg. 199 (2010) 2765–2778.
[36] C. Miehe, L.-M. Schänzel, H. Ulmer, Phase field modeling of fracture in multiphysics problems. Part I. Balance of crack surface and failure criteria for brittle crack propagation in thermo-elastic solids, Comput. Methods Appl. Mech. Engrg. 294 (2015) 449–485.
[37] Q. Wang, W. Zhou, Y.T. Feng, The phase-field model with an auto-calibrated degradation function based on general softening laws for cohesive fracture, Appl. Math. Model. 86 (2020) 185–206.
[38] Q. Wang, Y.T. Feng, W. Zhou, Y.G. Cheng, G. Ma, A phase-field model for mixed-mode fracture based on a unified tensile fracture criterion, Comput. Methods Appl. Mech. Engrg. 370 (2020) 113270.
[39] F. Fei, J. Choo, A phase-field model of frictional shear fracture in geologic materials, Comput. Methods Appl. Math. 3691 (2020) 113265.
[40] S.W. Zhou, X.Y. Zhuang, T. Rabczuk, Phase field modeling of brittle compressive-shear fractures in rock-like materials: A new driving force and a hybrid formulation, Comput. Methods Appl. Math. 355 (2019) 729–752.
[41] G. Zhang, T.F. Guo, S. Tang, W.K. Liu, Fracture in tension-compression-asymmetry solids via phase field modeling, Comput. Methods Appl. Math. 357 (2019) 112573.
[42] S. Tang, G. Zhang, T.F. Guo, X. Guo, W.K. Liu, Phase field modeling of fracture in nonlinearly elastic solids via energy decomposition, Comput. Methods Appl. Math. 347 (2019) 477–494.
[43] S.W. Zhou, X.Y. Zhuang, T. Rabczuk, A phase-field modeling approach of fracture propagation in poroelastic media, Eng. Geol. 240 (2018) 189–203.
[44] R.U. Patil, B.K. Mishra, I.V. Singh, T.Q. Bui, A new multiscale phase field method to simulate failure in composites, Adv. Eng. Softw. 126 (2018) 9–33.
[45] S.K. Singh, I.V. Singh, B.K. Mishra, G. Bhardwaj, T.Q. Bui, A simple, efficient and accurate Bézier extraction based T-spline XIGA for crack simulations, Theor. Appl. Fract. Mech. 88 (2017) 74–96.
[46] D.K. Thai, T.M. Tu, T.Q. Bui, T.T. Bui, Gradient tree boosting machine learning on predicting the failure modes of the RC panels under impact loads, Eng. Comput. (2019) http://dx.doi.org/10.1007/s00366-019-00842-w.
[47] S.Z. Feng, X. Han, Z.J. Ma, Grzegorz Królczyk, Z.X. Li, Data-driven algorithm for real-time fatigue life prediction of structures with stochastic parameters, Comput. Methods Appl. Math. 37 (2020) 113373.
[48] E. Samaniego, C. Anitescu, S. Goswami, V.M. Nguyen-Thanh, H. Guo, K. Hamdia, X. Zhuang, T. Rabczuk, An energy approach to the solution of partial differential equations in computational mechanics via machine learning: Concepts, implementation and applications, Comput. Methods Appl. Math. 362 (2020) 112790.
[49] S. Goswami, C. Anitescu, S. Chakraborty, T. Rabczuk, Transfer learning enhanced physics informed neural network for phase-field modeling of fracture, Theor. Appl. Fract. Mech. 106 (2020) 10244.
[50] A. Hjouji, J. El-Mekkaoui, M. Jourhmane, H. Qjidaa, B. Bouikhalene, Image retrieval and classication using shifted Legendre invariant moments and radial basis functions, Procedia Comput. Sci. 148 (2019) 154–163.
[51] A. Kumar, G. Vashishtha, C.P. Gandhi, Y.Q. Zhou, A. Glowacz, J.W. Xiang, Novel convolutional neural network (NCNN) for the diagnosis of bearing defects in rotary machinery, IEEE Trans. Instrum. Meas. 70 (2021) 3510710.
[52] A. Glowacz, Fault diagnosis of electric impact drills using thermal imaging, Measurment 171 (2021) 108815.
[53] B.A. Olshausen, D.J. Field, Emergence of simple-cell receptive field properties by learning a sparse code for natural images, Nature 381 (1996) 607–609.
[54] Y. Bengio, A. Courville, P. Vincent, Representation learning: A review and new perspectives, IEEE Trans. Pattern Anal. Mach. Intell. 35 (2013) 1798–1828.
[55] X. Li, Z.L. Liu, S.Q. Cui, C.C. Luo, Z. Zhuang, Predicting the effective mechanical property of heterogeneous materials by image based modeling and deep learning, Comput. Methods Appl. Mech. Engrg. 347 (2019) 735–753.
[56] P.C. Tripathi, S. Bag, CNN-DMRI: A convolutional neural network for denoising of magnetic resonance images, Pattern Recognit. Lett. 135 (2020) 57–63.
[57] Philip K. Kristensen, Emilio Martínez-Pañeda, Phase field fracture modelling using quasi-Newton methods and a new adaptive step scheme, Theor. Appl. Fract. Mech. 107 (2020) 102446.
[58] Y. LeCun, L. Bottou, Y. Bengio, P. Haffner, Gradient-based learning applied to document recognition, Proc. IEEE (1998).
[59] A. Kumar, C.P. Gandhi, Y.Q. Zhou, R. Kumar, J.W. Xiang, Improved deep convolution neural network (CNN) for the identification of defects in the centrifugal pump using acoustic images, Appl. Acoust. 167 (2020) 107399.
[60] G. Molnár, A. Gravouil, 2D and 3D abaqus implementation of a robust staggered phase-field solution for modeling brittle fracture, Finite Elem. Anal. Des. 130 (2017) 27–38.